Hindawi
Complexity
Volume 2024, Article ID 4933311, 17 pages
https://doi.org/10.1155/2024/4933311

Research Article

Research on Path Optimization of Vehicle-Drone Joint Distribution considering Customer Priority

Xiaoye Zhou and Yuhao Feng

School of Management, Shenyang University of Technology, Shenyang 110870, China

Correspondence should be addressed to Yuhao Feng; yfeng@smail.sut.edu.cn

Received 11 November 2023; Revised 16 December 2023; Accepted 30 December 2023; Published 10 January 2024

Academic Editor: Qingling Wang

To meet the personalized distribution needs of customers, comprehensively consider customer value, the urgency of customer needs, and the impact of priority distribution to the customer on the enterprise, and based on regional restrictions, put forward vehicle-drone joint distribution path optimization problem considering customer priority. First, the goal is to minimize the sum of total distribution cost and customer priority cost integrating soft time windows and constructing a path optimization model of the vehicle-drone joint distribution. Second, a two-stage hybrid algorithm is proposed for the problem model. In the first stage, the deep neural network and the grid search improved support vector machine algorithm (DNN-GSM-SVM) are used to screen and classify customer priority features, and in the second stage, adaptive large-scale neighborhood search improved genetic algorithms (ALNS-GA) are used to solve the problem of vehicle-drone joint distribution path planning problem. Finally, combined with the numerical example, the optimization scheme of the vehicle-drone joint distribution path considering priority is analyzed. Compared with the three algorithms and error analysis, the effectiveness of the model and the two-stage algorithm was verified. Compared with the results of the scheme that does not consider priority, the results show that priority can significantly improve customer satisfaction. The efficiency of the vehicle-drone joint distribution was verified by comparing the three scenarios.

1. Introduction

With the rapid development of the digital economy, the deep integration of the digital economy and the real economy has become the main trend. Drones are an essential part of the digital economy and are increasingly valued in the market owing to their fast, low-cost, and unrestrained terrain characteristics. At this stage, with limited resources, different customers can bring different word-of-mouth impacts and profits to enterprises. Therefore, meeting the personalized needs of customers has become a key research direction for logistics enterprises. At present, most of the end distribution of logistics companies has adopted a single form of vehicle distribution, which has disadvantages such as high costs and incomplete customer coverage. These opportunities and challenges have prompted a shift from traditional vehicle distribution to the vehicle-drone joint distribution model at the current end distribution, while further considering customer priority levels and prioritizing meeting the time window requirements of high-level customers. The above shows that the path optimization of vehicle-drone joint distribution considering customer priority is of reference significance for the development of logistics enterprises and improves the common interests of consumers, e-commerce companies, and logistics companies.

2. Literature Review

2.1. Research on Vehicle-Drone Joint Distribution. In recent years, drone distribution has attracted the attention of domestic and foreign scholars owing to its efficiency and low-cost advantages. For example, Murray and Chu first proposed joint distribution mode of trucks and drones [1]. Chang and Lee proposed a new approach on a nonlinear programming model to cluster customers and research vehicle support for drone distribution, but without considering the time window [2]. Ha et al. considered the mode of each truck with a drone problem, the objective was to minimize total transportation costs, and one created by waste time a vehicle has to wait for the other, but without considering multiple trucks and drones for delivery [3]. Boysen et al. differentiated whether each vehicle was equipped with multiple drones or one drone and whether or not take-off and landing stops have to be identical [4]. Ham studied the vehicle-drone parallel distribution, considering two different types of drone tasks: drop and pickup, without considering vehicle capacity [5]. Karak and Abdelghany used a vehicle as an auxiliary tool for drones, the drone completed all the distribution services, while considering the flight distance and carrying capacity limitations of drones, and and improved Clarke–Wright algorithm was designed to solve the problem [6]. Wang and Lan proposed that the customer points near the expressway be delivered by drones. The remaining customers within the city are serviced by vehicles [7]. Moshref-Javadi et al. considered the carrying capacity and endurance limits of drones, and an efficient hybrid Tabu Search-Simulated Annealing algorithm was developed to solve the problem [8]. Schermer et al. introduced a robot station in the vehicle-drone joint distribution mode and designed a mixed integer linear programming formulation to solve the problem without considering the impact of multiple trucks [9]. Salama and Srinivas proposed two clustering strategies to determine drone docking point: one strategy was to restrict it to one of the customer locations and the other one was to allow it to be anywhere in the delivery area [10]. Han et al. proposed a three-objective optimization model of minimum vehicle energy consumption, minimum drone energy consumption, and minimum vehicle quantity [11]. Peng and Lai divided customers into three categories: those who are only served by vehicles, those who are only served by drones, and those who are jointly delivered by vehicles and drones [12]. Dayarian et al. proposed that drones support vehicle distribution. The role of drones is to supply vehicle, and the potential benefits of drone resupply are quantified, but without considering vehicle capacity and drone travel range [13]. Liu et al. designed three types of drone-vehicle distribution scenarios, and drones can serve multiple customer points with each delivery [14]. Yan et al. studied emergency logistics and considered regionally limited vehicles equipped with drone path problems [15]. Yang et al. used the COVID-19 isolation period as the background and adopted a three-stage solution method to effectively solve the problem of contactless distribution [16]. Zhang and Li considered the vehicle-drone path planning problem of fresh distribution during an epidemic [17]. Windras et al. introduced charging stations to charge vehicles and drones and served as launch and retrieve points for drones. To solve the problem, a memetic algorithm-based approach with four new problem-specific operators was developed [18]. Wang et al. worked on vehicle-drone routing systems with the goal of minimum time, and then they derived a number of worst-case results. The conclusion is that the worst-case results depend on the number of drones per truck and the speed of the drones relative to the speed of the truck [19]. Poikonen et al. studied the vehicle-drone considering the different indicators between vehicles and made connections with another practical variant of the vehicle routing problem and with Amdahl's Law [20]. Schermer et al. proposed an extension of the Vehicle Routing Problem with Drones (VRPDs) called the Vehicle Routing Problem with Drones and En Route Operations (VRPDEROs); drones may not only be launched and retrieved at vertices but also on some discrete points that are located on each arc, and a hybrid variable domain search algorithm is designed to solve the vehicle-drone delivery problem, but without considering the time windows [21]. Popovic et al. established a three-index mixed integer quadratic programming formula to study vehicle-drone delivery [22]. Sacramento et al. proposed the MLP formula to further study the vehicle-drone delivery problem and considered time limit constraints. Moreover, a detailed sensitivity analysis is performed on several drone parameters of interest [23]. Kuo et al. aimed to minimize total delivery costs, and the MIP formula is proposed to study the vehicle-drone delivery problem with a time window [24]. Murray and Raj designed the MILP formula, considering the importance of appropriate scheduling of pickup and delivery services within a single customer node. Although the study considered drones of differing capacities, there was no analysis regarding the impact of these capacities [25]. Zhu et al. studied the electric vehicle-drone traveling salesman problem, and a three-index MILP formulation was proposed to solve the problem [26]. Kyriakakis et al. studied electric car-assisted drones for customer service, with electric vehicles not involved in direct delivery [27]. Windras Mara et al. considered a drone was capable of visiting multiple customer nodes within a single sortie and proposed a new mathematical formulation and a new heuristic approach based on adaptive large neighborhood search (ALNS) [28].

From the perspective of distribution modes, the above literature can be divided into vehicle-drone joint distribution mode, drone assisted by vehicle distribution mode, and vehicle drone parallel distribution mode; from the perspective of the number of drones carried, it can be divided into two categories: each vehicle can carry one and multiple drones; from the perspective of whether to consider time windows, it can be divided into considering time windows and not considering time windows. However, in this literature, scholars assumed that the drone could only deliver a customer once in flight and could not visit multiple customers within a single sortie, which was too simplified and reduced the efficiency of drone use, which was not in line with the reality. In addition, most scholars only consider the time window limit of customers and lack detailed research on customers' individual needs. This study will improve the above deficiencies.

2.2. Research on Priority. Owing to the increasing emphasis on personalized customer needs and a gap in the supply and demand ratio, customer priority problems have been widely applied in distribution target tasks. The quality of logistics services can be improved by studying the distribution order of customers, and distribution delays can be reduced. Therefore, many scholars have conducted in-depth research on priority issues in various aspects and achieved relatively rich research results.

De Souza et al. established a hypercube model based on spatial distribution queue theory to analyse systems with multiple priorities, waiting queues for customers, and processed customer priority queue sequences [29]. Lee et al. divided customers into ordinary and picky customers using data envelopment analysis, taking into account the expected levels and service perceptions [30]. To determine the distribution priority of emergency supplies, Schreiber used the Analytic Hierarchy Process (AHP) to apply a consistent fuzzy preference relationship to the decision matrix, and used the symmetric decision matrix method [31]. Wang et al. introduced variable weight factors in the Analytic Hierarchy Process (AHP) to enable experts to assign weights to sustainable development indicators that can vary over time or space. They proposed a new and improved weight allocation method called the variable weight Analytic Hierarchy Process (VWAHP), which can better reflect the true state of indicators [32]. The entropy method is a commonly used weighting method for measuring value dispersion in decision-making. The greater the degree of dispersion, the greater the degree of differentiation, and more information can be derived. At the same time, the indicator should be given a higher weight and vice versa. Shrestha proposed a factor analysis method that uses the Kaiser–Meyer–Olkin sampling adequacy measure and Bartlett's sphericity test to evaluate the decomposability of the data [33].

In summary, there was no consideration of customer priority in previous studies on the vehicle-drone joint distribution, and customer priority became the current research hotspot because it could meet consumer individual needs. This study comprehensively considers customer priority, vehicle-drone joint distribution mode, and regional restrictions, integrates soft time windows into customer priority, establishes priority cost models, and proposes a vehicle-drone joint distribution considering customer priority problem. The two-stage hybrid optimization algorithm framework is designed as follows:

The first-stage optimization algorithm is the deep neural network, grid search improved support vector machine algorithm (DNN-GSM-SVM). Using DNN to wake up data dimensionality reduction can reduce redundant data, improve computational efficiency, and reduce the risk of model overfitting. Compared with the traditional AHP algorithm, the GSM-SVM algorithm can process a large number of index data, and this method belongs to supervised machine learning, which can further predict the future and provide new solutions.

The second stage optimization algorithm is an adaptive large-scale neighborhood search improved genetic hybrid algorithm (ALNS-GA) to solve customer level classification and vehicle-drone path optimization problems. Compared with the traditional adaptive genetic algorithm (AGA), ALNS-GA increases the trade-off of operator effectiveness and evaluates the operator based on the quality of new solutions found. Dynamically update the operator weights and use the roulette wheel method to select a set of operators to destroy and repair the current solution.

3. Problem Description and Mathematical Model

3.1. Problem Description. Vehicle Routing Problem with Vehicle-Drone Considering Customer Priority (VRP-VDCCP). As shown in Figure 1, each vehicle is equipped with a drone departing from the distribution center, both of which can deliver goods to customers. In the distribution process, regional restrictions and customer priorities are further considered, and priority is given to meet the time window requirements of higher-level customers. At the same time, it is stipulated that some customer points are located in the vehicle restricted area and the drone no-fly area. Customer points located in the vehicle restricted area can only be delivered by drones, and customer points located in the drone no-fly area can only be delivered by vehicles. The VRP-VDCCP problem can be seen as an integration of two subproblems: Customer Priority Classification (CPC) and Vehicle Routing Problem with Vehicle and Drone (VRP-VD). The CPC problem involves reasonably selecting the main influencing features from numerous features that affect customer priority and then classifying customers based on the selected features. The VRP-VD problem includes two types of distribution routes: the route of vehicles from the distribution center to customer points and the route of drones taking off from the distribution center or from vehicles to customer points.

3.2. Mathematical Model

3.2.1. Model Assumptions. This article makes the following assumptions about the VRP-VDCCP problem:

(1) Each vehicle can carry a drone, which can visit multiple customers within a single sortie
(2) The drone can depart and return from the distribution center independently
(3) Drones and vehicles are not allowed to have subcircuits
(4) Both the drone and the vehicle are traveling at a constant speed
(5) Do not consider the charging and unloading time of drones
(6) Vehicles and drones are homogeneous
(7) The drone cannot fly into the no-fly area, and the vehicle cannot drive into a restricted area

3.2.2. Customer Priority Cost Function Integrating Soft Time Window. In logistics distribution services, whether high-level customers can obtain the service on time is a key factor that affects the cost of customer priority. In reality, customer requirements for time windows are not rigid but have a certain space for flexible adjustment. Therefore, this study constructs a relationship based on soft time windows and priority cost as shown in Figure 2.

In Figure 2, t_i is the time to reach customer i, $[ET_i, LT_i]$ is the soft time window range for customer i, when $n = 1, 2, 3$

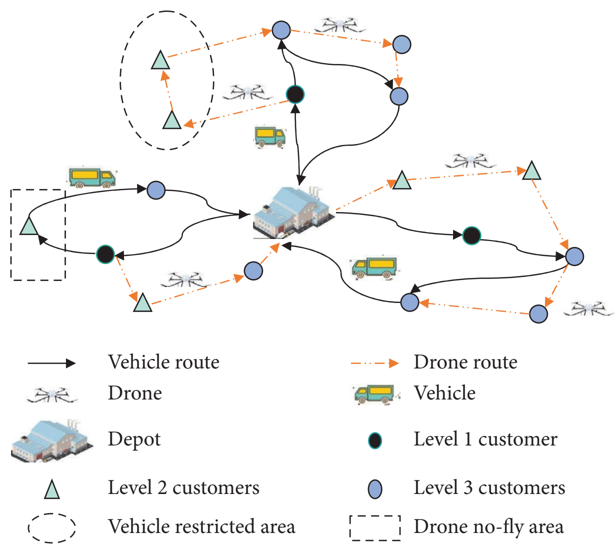

FIGURE 1: Distribution path with different priority modes.

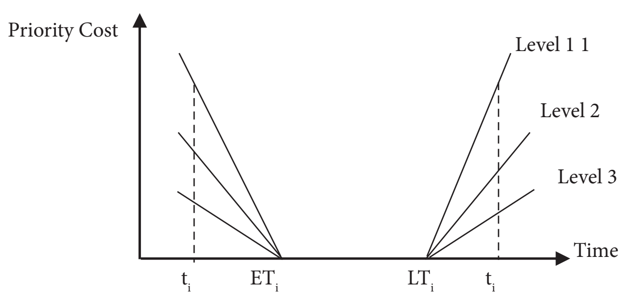

FIGURE 2: Soft time window with different priority cost relationship.

denote $\theta_1 = 1$ for the customer of level 1 priority distribution, $\theta_2 = 2$ for the customer of level 2, and $\theta_2 = 3$ for the customer of level 3, respectively. Based on the soft time window with priority cost function, as in equation (1), it can be seen that the cost coefficients for violating the time windows of level 1, level 2, and level 3 customers are 1000, 100, and 10, respectively.

$$R_i(t_i) = \begin{cases} 10^{4-\theta_n}(t_i - \mathrm{ET}_i), & t_i \le \mathrm{ET}_i, \\ 0, & \mathrm{ET}_i \le t_i \le \mathrm{LT}_i, \\ 10^{4-\theta_n}(t_i - \mathrm{LT}_i), & \mathrm{LT}_i \le t_i. \end{cases} \quad (1)$$

3.2.3. Mathematical Model. Vehicle Routing Problem with Vehicle-Drone Considering Customer Priority (VRP-VDCCP) network is described as a graph-theoretic problem, such that $G = (V, A)$ is an undirected noncomplete graph, where $V = \{0, 1, 2, \ldots, n\}$ denotes the set of nodes and $A = \{(i, j) \mid i, j \in V\}$ denotes the set of arcs. Node 0 denotes the distribution center, the remaining nodes represent customers, and the set of customers is denoted by $V_c = \{0, 1, 2, \ldots, n\}$. A_T denotes the set of arcs in which vehicles can travel, and A_D denotes the set of arcs in which drones can fly. The distribution center has several same type vehicles, and each vehicle carries a drone of the same type. The maximum load weight of vehicle is GT, the maximum load weight of drone is GD, and the longest single flight distance of drone is LD. The relevant symbols used in the model are defined in Tables 1–3.

$$\min F = F_1 + F_2, \quad (2)$$

$$\min F_1 = f_1 + f_2, \quad (3)$$

$$\min F_2 = f_3 \cdot f_4, \quad (4)$$

$$f_1 = C_0 \sum_{i\in V} \sum_{j\in V} \sum_{s\in \mathrm{Vs}} d_{ij} \cdot x_{ij}^s + C_1 \sum_{i\in V} \sum_{j\in V} \sum_{s\in \mathrm{Vs}} d'_{ij} \cdot z_{ij}^s, \quad (5)$$

$$f_2 = \mathrm{FC}_0 \sum_{S\in \mathrm{Vs}} \mathrm{pt}^s + \mathrm{FC}_1 \sum_{S\in \mathrm{Vs}} \mathrm{pd}^s, \quad (6)$$

$$f_3 = \sum_{i\in V} p_i(t_i), \quad (7)$$

$$f_4 = 10^{4-\theta n}. \quad (8)$$

Equations (2)–(8) are objective functions and equation (2) represents the minimum total cost. Equation (3) represents the minimum distribution cost. Equation (4) represents the minimum priority cost. Equations (5)–(8) represent the travel and flight cost, fixed cost, penalty cost, and priority cost coefficients, respectively, subject to

$$u_i^s = \sum_{j\in \mathrm{Vc}} \left(x_{ij}^s + x_{ji}^s\right), \quad \forall i \in \mathrm{Vc}, \forall s \in \mathrm{Vs}, \quad (9)$$

$$v_i^s = \sum_{i\in \mathrm{Vc}} \sum_{j\in V} z_{ij}^s, \quad \forall s \in \mathrm{Vs}, \quad (10)$$

$$\sum_{s\in \mathrm{Vs}} \left(u_i^s + v_i^s\right) = 1, \quad \forall i \in V, \quad (11)$$

$$\sum_{i\in V} x_{0i}^s = \sum_{i\in V} x_{i0}^s = 1, \quad \forall i \in \mathrm{Vc}, \forall s \in \mathrm{Vs}, \quad (12)$$

$$\sum_{i\in V} \sum_{j\in V} x_{ij}^s \le \left(1 - \frac{1}{M}\right) \cdot \sum_{i\in \mathrm{Vc}} u_i^s + 1, \quad \forall s \in \mathrm{Vs}, \quad (13)$$

$$\sum_{i\in \mathrm{Vc}} \sum_{j\in V} z_{ij}^s \le 1, \quad \forall i, j \in V, \forall s \in \mathrm{Vs}, \quad (14)$$

$$\sum_{j\in V} x_{ij}^s = \sum_{j\in V} x_{ji}^s \le 1, \quad \forall i \in V, \forall s \in \mathrm{Vs}, \quad (15)$$

$$x_{ij}^s \ge z_{ij}^s, \quad \forall i, j \in V, \forall s \in \mathrm{Vs}, \quad (16)$$

Table 1: Assembles.

Symbol	Definition
$V_c = \{1, 2, \ldots, n\}$	Set of all customer nodes
$V = V_c \bigcup \{0\}$	Set of all nodes, {0} indicates distribution center
V_s	Set of vehicles

Table 2: Parameters.

Symbol	Definition
FC_0	A vehicle fixed cost
FC_1	A drone fixed cost
C_0	Vehicle unit travel cost
C_1	Drone unit flight cost
GT	Vehicle load limit
GD	Drone load limit
LD	The farthest distance a drone can fly in a single trip
θ_i	Priority of point i
V_t	Vehicle travel speed
V_d	Drone flight speed
d_{ij}	Travelling distance of the vehicle from i to j
d'_{ij}	Flight distance of the drone from i to j
q_i	Customer i demand
M	A large enough positive integer
gd_{ij}	The path from i to j does not pass through the no-fly area
gt_{ij}	The path from i to j does not pass through the restricted area

$$\sum_{i\in V} q_i \cdot u_i^s + \sum_{i\in V} q_i \cdot v_i^s \leq \mathrm{GT}, \quad \forall s \in V_s, \tag{17}$$

$$q_i \cdot v_i^s \leq \mathrm{GD}, \quad \forall i \in \mathrm{Vc}, \forall s \in \mathrm{Vs}, \tag{18}$$

$$x_{ij}^s \leq \mathrm{gt}_{ij}, \quad \forall i, j \in V, \forall s \in \mathrm{Vs}, \tag{19}$$

$$x_{ij}^s \leq \mathrm{gd}_{ij}, \quad \forall i, j \in V, \forall s \in \mathrm{Vs}, \tag{20}$$

$$d'_{ij} \cdot z_{ij}^s \leq \mathrm{LD}, \quad \forall s \in \mathrm{Vs}. \tag{21}$$

Constraints (9) and (10) indicate the relationships between the decision variables, which substantially simplify the model. Constraint (11) indicates that all customers can be served only once. Constraint (12) indicates that the vehicle departs from the distribution center and finally returns to the distribution center. Constraint (13) indicates that all vehicle paths do not allow for subloops. Constraint (14) indicates that all drone paths do not allow for subloops. Constraint (15) indicates that the vehicle can serve only one customer simultaneously. Constraint (16) indicates that the drone can visit multiple customers within a single sortie. Constraint (17) indicates a vehicle load constraint. Constraint (18) indicates the drone load constraint. Constraint (19) indicates that the vehicle path cannot pass through a restricted area. Constraint (20) indicates that the drone flight path cannot pass through the no-fly area. Constraint (21) represents the drone flight distance.

4. Algorithm Design

The VRP-VDCCP is an NP-hard problem. Combining the model characteristics and problem features, this article adopts a two-stage approach to divide the VRP-TDCCP into CPC and VRP-VD. The DNN-GSM-SVM algorithm is designed for priority feature screening and classification of customers to achieve the initial optimization in the VRP-VDCCP logistics network. Then, the ALNS-GA algorithm is used for vehicle-drone path optimization. The two-stage algorithm optimization framework is shown in Figure 3.

4.1. Customer Priority Classification Based on DNN-GSM-SVM Algorithm. Before the path optimization, the DNN was used to screen the initial customer priority indicators, and then the GSM-SVM was used to classify the customer priority according to the filtered features. The specific method of GSM-improved SVM is to divide the penalty function C and the kernel function g into grids within a specified range and traverse all points within the grid to take values; for the specified C and g, the K-order cross-validation method is used to obtain the classification accuracy of this set of C and g under the training set, and C and g with the highest classification accuracy of the training set were obtained as the best generated parameter set. The specific process is shown in Figure 4.

4.2. ALNS-GA for Solving Path Optimization. The genetic algorithm is a kind of algorithm idea that imitates the biological evolution process. It firstly encodes customers, then randomly generates the initial population, and calculates the fitness value of each individual. It goes through the genetics of replication, mutation, and crossover. After many iterations of the problem, finally, it generates the optimal solution or the approximate optimal solution. However, simpler algorithms based on the use of the adaptive large-scale neighborhood search often show better results within the same computation time. The generated customer priority classification is used as the input and applied to the solution path of the improved genetic algorithm for an adaptive large-scale neighborhood search. In this study, the variational operation of the traditional GA is followed by an adaptive large-scale neighborhood search operation to obtain the optimal solution. The specific steps are as follows.

4.2.1. Two-Stage Generation of Initial Solutions

Stage 1: First, the initial vehicle path is constructed without considering the drone and vehicle restricted areas.

Step 1: Select any customer from all customer points $j \in \{1, 2, \cdots, n\}$.
Step 2: Initialize the number of vehicles k is 1.
Step 3: Generate a sequence $\mathrm{seq} = \{j, j+1, \cdots, n, 1, \cdots, j-1\}$.
Step 4: From serial number i, keep looping to n, that is, generate the original solution, traverse customer seq

Table 3: Variables.

Symbol	Definition
$\mathrm{pt}^s = \{1, 0\}$	Binary variable: 1, if a vehicle s is enabled; 0, otherwise
$\mathrm{pd}^s = \{1, 0\}$	Binary variable: 1, if a drone s is enabled; 0, otherwise
$u_i^s = \{1, 0\}$	Binary variable: 1, if customer i is delivered by vehicle s; 0, otherwise
$v_i^s = \{1, 0\}$	Binary variable: 1, if customer i goods are delivered by drones carried by vehicle s; 0, otherwise
$x_{ij}^s = \{1, 0\}$	Binary variable: 1, if vehicle s from i to j; 0, otherwise
$z_{ij}^s = \{1, 0\}$	Binary variable: 1, if vehicle s carrying drone from i to j; 0, otherwise
$p_i(t_i) = \begin{cases} \partial(t_i - \mathrm{ET}_i) & t_i \leq \mathrm{ET}_i \\ 0 & \mathrm{LT}_i \leq t_i \leq \mathrm{ET}_i \\ \delta(t_i - \mathrm{LT}_i) & \mathrm{LT}_i \leq t_i \end{cases}$	Relationship between soft time window and satisfaction loss function

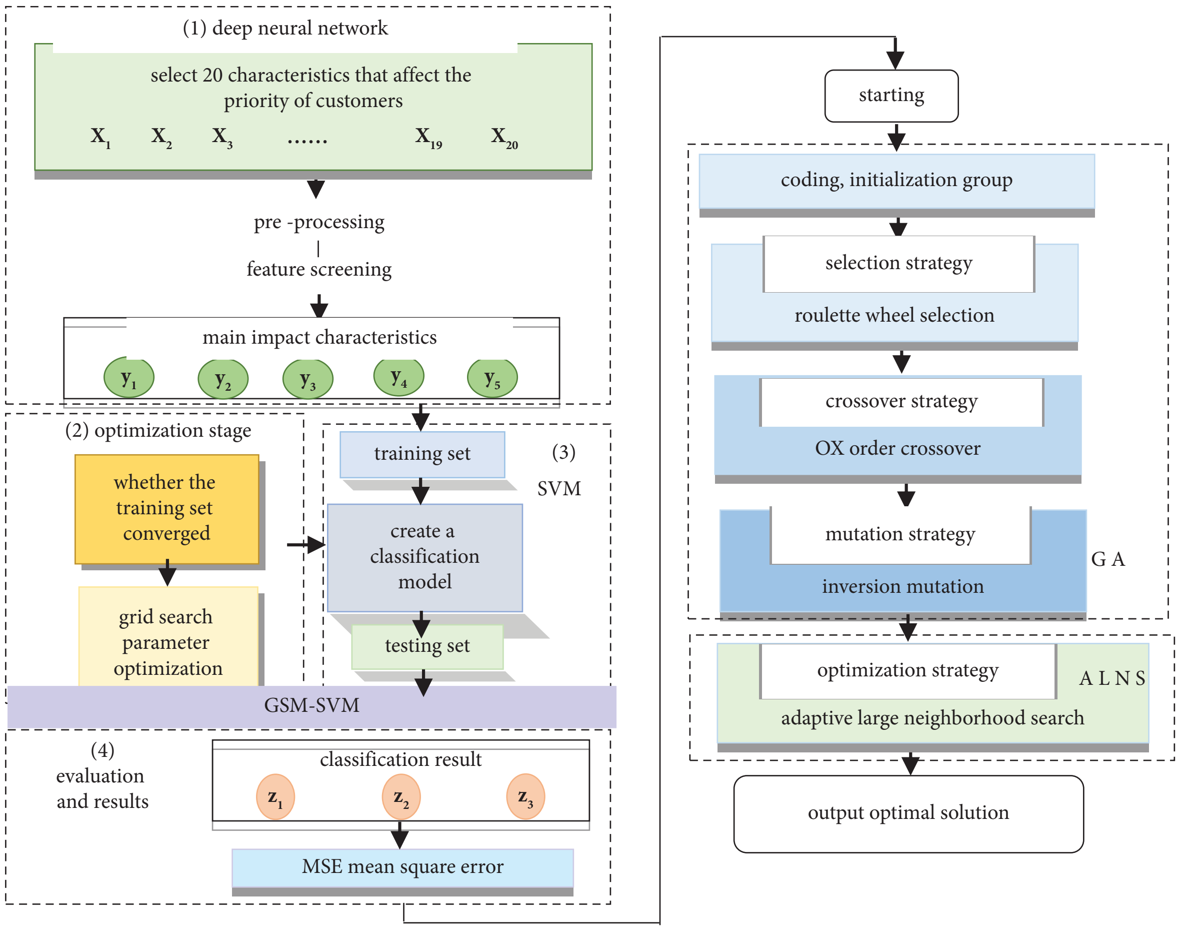

Figure 3: Two-stage algorithm optimization framework.

(i), place customer seq (i) into the k-th path, and divide it into two cases.

(1) If the k-th path does not reach the load limit, there are three scenarios: if there is no customer point in the current path, place sequence i into the path; if there is a customer in the current path, put the new customer i according to the left time window; if the current number of customers $l > 1$, traverse $l - 1$ pairs of customers.
(2) Confirm whether there is a position that can be inserted, if not, put it at the end.
(3) If the k-th path has reached the load limit, save the customers visited by the k-th vehicle. Then, update k to $k+1$.

Stage 2: Based on the generated vehicle paths, the drone paths are decomposed, and area restrictions are considered.

In the generated vehicle path, the value of the time variation for each customer satisfying the drone load and flight distance to be delivered by the drone, compared to distribution by vehicle, is calculated in the following equation:

$$\Delta t = \frac{d'_{ij} + d'_{ji}}{v_t} - \frac{d'_{ij} + d'_{ji}}{v_d}. \tag{22}$$

The customer with the greatest reduction in delivery time on each initial route are set to be served by drones, where Δt is set to infinity if customer point is in a restricted area or in a no-fly area. Update all routes until the route scheme no longer changes.

4.2.2. Calculation of the Fitness Function. To prevent decoding of each path from violating the priority and region restriction constraints, a cost function, such as equation (23), was used as the fitness function.

$$f(s) = c(s) + \alpha \cdot q(s) \cdot w(s), \tag{23}$$

where $c(s)$ represents the distribution cost of the vehicle and drone, $q(s)$ represents the customer priority cost constraint, and $w(s)$ represents the sum of the violation of the soft time window constraint. Because the adaptation degree value is ultimately selected out of the large one, the smaller the corresponding cost function, the better, so the fitness function is set as the inverse of the cost function.

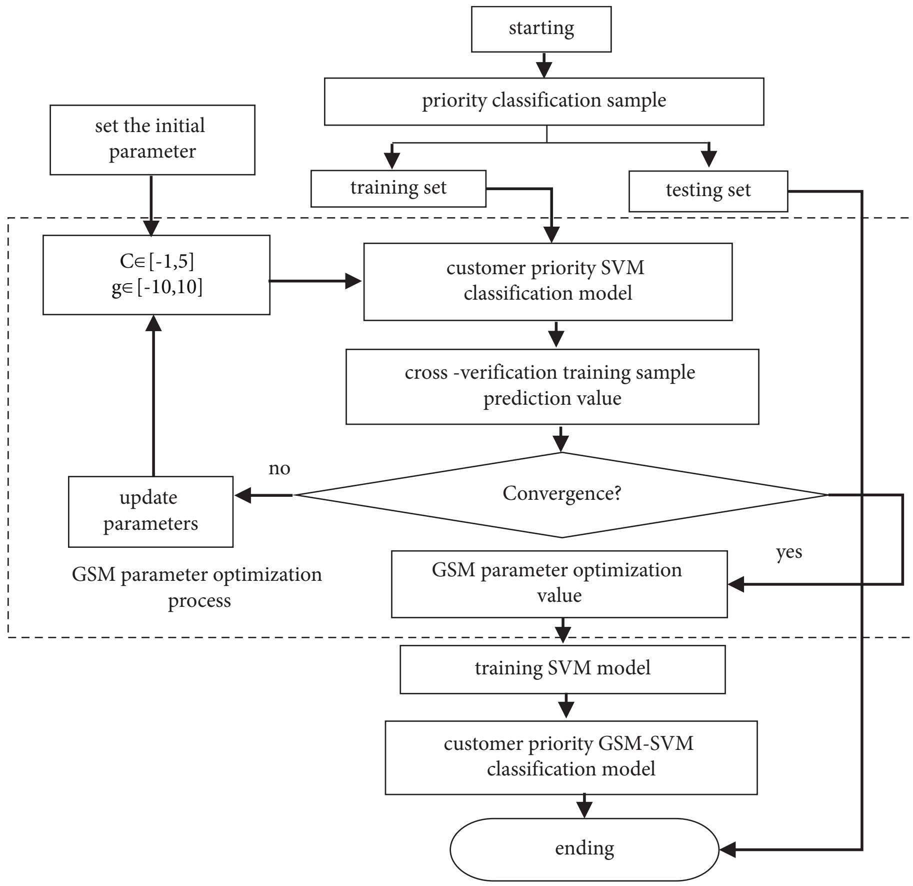

Figure 4: Grid search improved support vector machine flow chart.

4.2.3. Selection Operation. This section uses roulette wheel selection to select individuals with large fitness values according to their fitness values for crossover, variation, and local search operations.

4.2.4. Crossover Operation. This section designs the order crossover (OX) operator as shown in Figure 5, which generates two crossover fragments by randomly selecting the start and end positions in the two parent chromosomes, moving the crossover fragment of parent 1 to the front of parent 2, and moving the fragment of parent 2 to the front of parent 1. Duplicate codes in the noncrossover fragment were deleted in the generated new parent to create offspring.

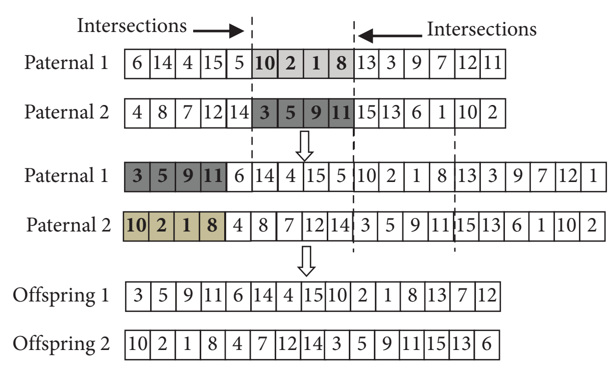

Figure 5: Schematic diagram of the crossover strategy.

4.2.5. Mutation Operation. The mutation operation can be analogous to the behavior of chromosomal mutations during gene inheritance and can affect the local search ability of the algorithm. A chromosome is randomly selected as a mutated individual; multiple mutation points are generated for swapping as shown in Figure 6.

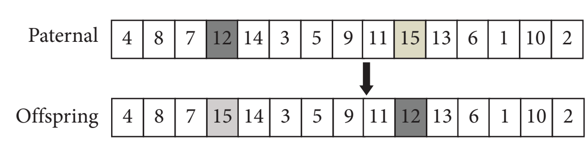

Figure 6: Schematic diagram of the mutation strategy.

4.2.6. Adaptive Large-Scale Neighborhood Search Operation. The traditional large-scale neighborhood search operation removes several customers from the solution using the destruction operator and then reinserts the removed customers back into the destroyed solution by using the repair operator. Similarly, when inserting, the location is not randomly selected for insertion, but to meet the load constraints and time window constraints as far as possible, the removed customer is inserted back into the position of the minimum total distance of the vehicle.

This article adopts the idea of destruction and repair, designing multiple removal and insertion operators, each with a weight assigned. On the basis of ALNS, it increases the trade-off of operator effectiveness and evaluates the operator based on the quality of the new solutions found. Dynamically update the operator weights and use the roulette wheel method to select a set of operators to destroy and repair the current solution.

Based on the VRP-VD mathematical model, three removal operators and two reinsertion operators were designed. According to equation (24), R customers were removed each time.

$$R = \text{rand}i\left(\left[c_1 \times (N+1)\right], \left[c_2 \times (N+1)\right]\right). \tag{24}$$

Randi (x, y) represents the generation of a pseudorandom integer between x and y; N represents the total number of customers; c_1 and c_2 represent coefficients generated between (0, 1); and $[A]$ represents rounding A to the nearest whole number.

(1) Removal Operators. The random removal operator randomly removes R customers based on the current solution, while the correlation removal operator removes the node with the smallest correlation with the selected node. That is, randomly select one customer i_1 to remove, calculate the correlation D between the remaining customers and i_1 as in equations (25) and (26), and select the customer with the highest correlation for removal.

$$D(i,j) = \frac{1}{\left(d'_{ij} + v_{ij}\right)}, \tag{25}$$

$$d'_{ij} = \frac{d_{ij}}{\max\left(d_{\text{in}}\right)}. \tag{26}$$

v_{ij} indicates whether the customer is on the same path; 1 indicates yes, and 0 indicates no; and d_{ij} indicates the distance from customer i to j. The distances are all Euclidean distances.

In the removed customer set, randomly select one customer i_2, calculate the correlation between the remaining customers and i_2, and select the customer with the highest correlation for removal until the number of removed customers equals R.

The requirement-related removal operator is used to remove nodes with similar requirements to the selected node but not on the same route. The steps are as follows:

(1) Calculate the weight u of each path, select one path using the roulette wheel method, and randomly select one customer i to remove from that path. The path weight is shown in the following equation:

$$u = \sum_{i=1}^{n} q_i - \min \sum_{j=1}^{n} q_j + \lambda. \tag{27}$$

q_i is the demand for customer i; n is the number of all customers on the path; and λ is a very small positive number, preventing u from being 0.

(2) Calculate the demand correlation g between each path and i, and then use the roulette wheel method to sequentially remove the remaining R-1 customers. The correlation between all customer demands and i is shown in the following equation:

$$g == \frac{1}{\left(q - q_i\right)^2} + \varphi. \tag{28}$$

q is the demand of the customer; and φ is a very small positive number.

(2) Reinsertion Operators. The greedy insertion operator refers to sequentially inserting removed customers, each time satisfying capacity constraints, time window constraints, and the position with the smallest distance increment. If not, a new path is created to insert them. The minimum distance increment and maximum insertion operator are as follows:

(1) Identify the appropriate insertion point for each removed customer, which satisfies capacity constraints and time window constraints; if not, temporarily add it to a new path

(2) Calculate the distance increment of the appropriate insertion point for each customer and find the minimum distance increment

5. Numerical Experiments

To verify the applicability and effectiveness of VRP-VDCCP in the current environment, data from the Solomon dataset R201 were selected and applied to the calculations in this study. One distribution center has 34 customer points with known location coordinates, time windows, and demands. The relevant parameters were set as follows: $FC_0 = 100$, $FC_1 = 10$, $C_0 = 10$, $C_1 = 1$, $GT = 200$, $GD = 30$, $LD = 30$, $V_t = 60$ km/h, and $V_d = 80$ km/h; vehicles and drones departure time from the distribution center was 0, NIND = 100, MAXGEN = 500, $P_c = 0.9$, $P_m = 0.05$, and GGAP = 0.9. All algorithms were run on an AMD Ryzen 7 5700U with Radeon Graphics 1.80 GHz and 16.0 GB RAM computer using MATLAB R2022b.

5.1. Customer Priority Classification Based on DNN-GSM-SVM

5.1.1. Customer Priority Feature Screening Based on DNN

(1) DNN Model Input. In this study, we first used a deep neural network (DNN) to screen 20 features that affect customer priority as shown in Table 4 and selected the Relu function $\text{Logloss} = -1/N\sum_{i=1}^{N}(y \cdot \log p_i + (1-y) \cdot \log(1-p_i))$ as the activation function and loss function using the cross-entropy loss function, where p_i is the probability of the i-th sample predicted to be 1.

(2) DNN Model Output. The loss rate and accuracy rate obtained by DNN feature screening are shown in Figure 7, respectively. When there are no feature value indicators

Table 4: Initial characteristic index.

	Primary indicators	Secondary indicators
Customer priority level	Customer value	0: recent consumption
		1: consumption frequency
		2: attention level
		3: creditworthiness
		4: consumption strength
		5: activation
		6: comments on value
		7: accept consumption recommendations and successful consumption times
		8: forecast future purchases based on history
		9: whether it is a famous customer
		10: whether you are a VIP customer
		11: number of new customers referred
		12: whether to give good reviews after the sale
	Urgency of customer needs	13: accept the latest distribution time
		14: whether the expedited has been processed
		15: the delivery cycle is too long due to logistics reasons
		16: whether it is a special commodity
	Priority distribution of the impact of this customer to the enterprise	17: the benefits to the business
		18: the cost to the business
		19: whether to bring the enterprise backlog of goods

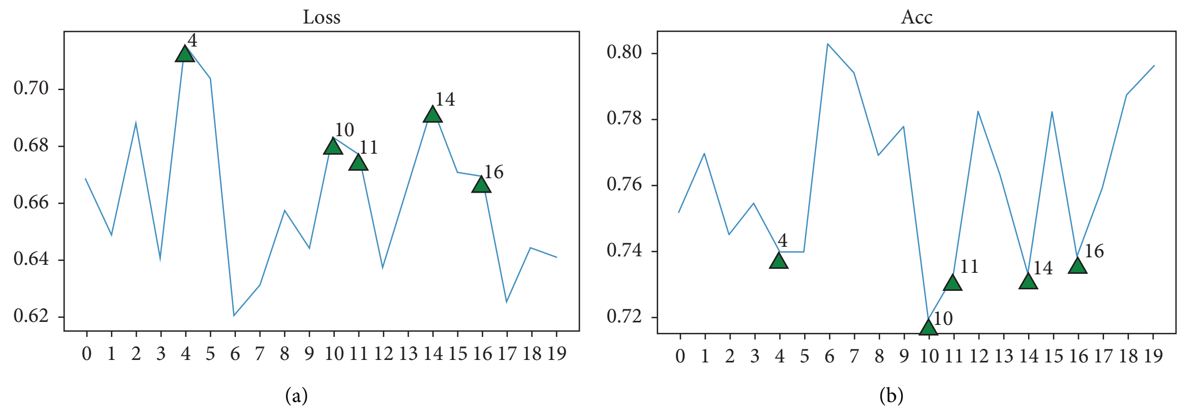

Figure 7: Screening feature indicator chart. (a) Feature screening loss rate graph. (b) Feature screening accuracy rate graph.

numbered 4, 10, 11, 14, and 16, the model loss value increases as shown in Figure 7(a). Conversely, the accuracy rate decreases as shown in Figure 7(b). It is proven that the five feature indicators corresponding to the consumption strength, whether it is a VIP customer, the number of recommended new customers, whether to handle expedited service, and whether it is a particular product (fresh products need to be refrigerated and other goods), have a great influence on the model, and the screening is completed.

5.1.2. Customer Priority Classification Based on GSM-SVM

(1) GSM-SVM Model Input. After screening 20 features affecting customer priority with DNN, the GSM improved SVM to classify customer priority in rank using the five screened features. In this study, 34 customer samples were selected; 26 groups of customers were randomly chosen as training sets, and the remaining eight groups were used as test sets. The screened 5 indicators were used as model input, and customer priority was used as the model output. The final result classifies the customers into three categories.

(2) Sample Standardization. This study uses normalized equation (29) to preprocess the input indicators of the SVM classification model.

$$X_i^* = \frac{(X_i - X_{\min})}{(X_{\max} - X_{\min})}, \quad (29)$$

where X_i and X_i^* are the i-th sample values of each indicator with their corresponding normalized values and $X_{\min}$ and $X_{\max}$ are the minimum and maximum values of each indicator, respectively.

(3) Parameter Search and Error Analysis. In this study, the parameters C and g of the SVM were optimized using the grid search method so that the values of C were in the range of (−1, 5) and g were in the range of (−10, 10).

To assess the accuracy of the model, the mean square error (MSE) was selected as the evaluation index in this study as shown in the following equation:

$$\text{MSE} = \frac{1}{N}\sum_{i=1}^{n}(y_i - \hat{y})^2. \quad (30)$$

When the MSE result is smaller, the prediction accuracy is higher. The final results of the parameters of the grid search optimization and the mean square error of the model in this study are shown in Figure 8, with the best $C = 24.2515$, $g = 0.25$, and $\text{MSE} = 0.1421$, which demonstrates that the model is highly accurate and strong in classification.

(4) GSM-SVM Model Outputs. The total number of samples selected in this study is 34, the number of samples in the training set is 26, and the number of samples in the test set is 8. The prediction results for the test set samples are shown in Table 5. The classification accuracy of GSM-SVM reached 87.5%, which is highly accurate, and the model is completed. The final priority ranks of 34 customers are shown in Table 6.

5.2. Vehicle-Drone Joint Distribution Results. The vehicle-drone joint distribution path, considering customer priority, is obtained by applying the ALNS-GA solution as shown in Figure 9. It is specified that the 23rd customer point in the restricted zone is the area where vehicles are not allowed to drive, and the 19th customer point in the no-fly zone is the area where drones are not allowed to fly. The optimized route results are shown in Tables 7 and 8.

To combine the optimization results of the two stages, the finalized customer priority classification is shown in Table 6, and the vehicle-drone joint distribution path is shown in Table 7. There are 6 customers of level 1, 8 customers of level 2, and 20 customers of level 3 in the entire distribution. Five vehicles are used, with each vehicle carrying one drone. For example, when vehicle 1 carries drone 1 for customer distribution, the vehicle 1 route is $0 \longrightarrow \text{C5} \longrightarrow \text{C16} \longrightarrow \text{C13} \longrightarrow 0$, while the drone 1 route is $\text{C5} \longrightarrow \text{C14} \longrightarrow \text{C16} \longrightarrow \text{C17} \longrightarrow \text{C13}$, drone 1 on vehicle 1 flies from C5 to C14 for distribution and rendezvous with vehicle 1 at C16; after charging and loading cargo, it takes off

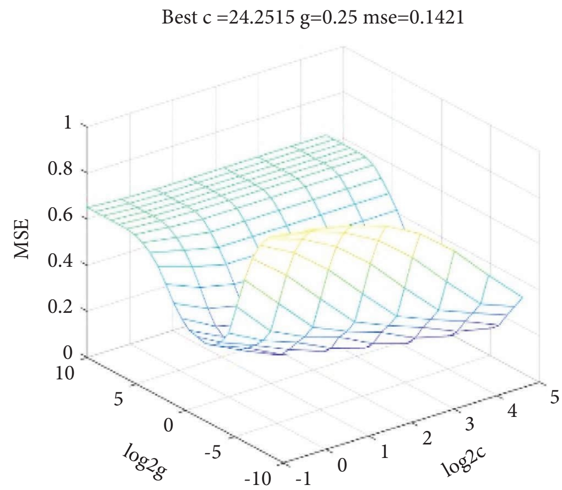

Figure 8: SVR parameter selection and MSE results.

Table 5: Test set sample prediction results.

Customer number	Priority true value	Priority forecast value	Correct rate (%)
4	3	3	100
7	3	3	100
18	3	3	100
19	3	1	0
22	3	3	100
26	3	3	100
33	3	3	100
34	3	3	100

Table 6: Customer priority ranking.

Customer	Priority	Customer	Priority	Customer	Priority
1	3	13	2	25	3
2	1	14	3	26	3
3	3	15	1	27	2
4	3	16	2	28	3
5	2	17	3	29	1
6	2	18	3	30	3
7	3	19	1	31	2
8	3	20	3	32	2
9	2	21	3	33	3
10	3	22	3	34	3
11	3	23	1		
12	1	24	2		

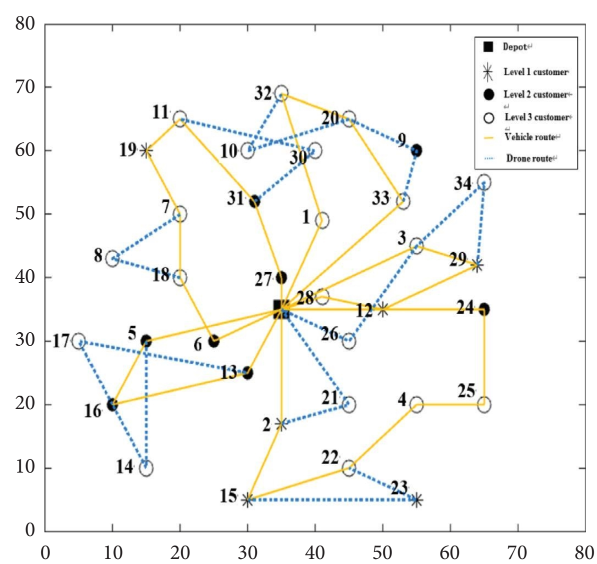

Figure 9: Vehicle-drone joint distribution path.

from C16 to C17 for distribution, and after distribution, drone 1 will rendezvous vehicle 1 at C13 and return to the distribution center together with vehicle 1. The total cost is 7581.0.

5.3. Algorithm Performance Analysis. Obtaining small-scale arithmetic based on the Solomon dataset and the effectiveness of the model and algorithm is illustrated by comparing the three algorithms. Five sets of arithmetic cases with 10, 15, 20, 25, and 30 customers are solved. The three metrics are used which are the total cost of the vehicle-drone distribution ($F1$), priority cost ($F2$), and solution time (t). According to Table 9, it can be seen that the ALNS-GA solution obtains better cost metrics than the traditional GA and GAA-GA algorithm solutions. In addition, the average solution time of the ALNS-GA algorithm is less than that of the traditional GA algorithm, which is only 0.09 more than that of the GAA-GA algorithm. The adaptation curves of the three algorithms are obtained as shown in Figure 10; the

Table 7: Vehicle-drone joint distribution path.

Truck	Vehicle route	Drone	Drone route
1	0 ⟶ C5 ⟶ C16 ⟶ C13 ⟶ 0	1	C5 ⟶ C14 ⟶ C16 ⟶ C17 ⟶ C13
2	0 ⟶ C2 ⟶ C15 ⟶ C22 ⟶ C4 ⟶ C25 ⟶ C24 ⟶ 0	2	0 ⟶ C21 ⟶ C2C15 ⟶ C23 ⟶ C22
3	0 ⟶ C28 ⟶ C12 ⟶ C29 ⟶ C3 ⟶ 0	3	C29 ⟶ C34 ⟶ C3 ⟶ C26 ⟶ 0
4	0 ⟶ C27 ⟶ C31 ⟶ C11 ⟶ C19 ⟶ C7 ⟶ C18 ⟶ C6 ⟶ 0	4	C31 ⟶ C30 ⟶ C11C7 ⟶ C8 ⟶ C18
5	0 ⟶ C33 ⟶ C9 ⟶ C32 ⟶ C1 ⟶ 0	5	C9 ⟶ C20 ⟶ C10 ⟶ C32

Table 8: Vehicle-drone joint distribution cost.

Number of vehicles used	Total vehicle distribution cost	Number of drones in use	Total drone distribution cost	Priority cost	Total cost
5	6039.9	5	371.4	1169.7	7581.0

Table 9: Comparison of results of GA, GAA-GA, and ALNS-GA algorithms.

Example	Number	GA			GAA-GA			ALNS-GA		
		*F*1	*F*2	*t*	*F*1	*F*2	*t*	*F*1	*F*2	*t*
1	10	3173.2	579.6	11.47	2992.3	467.6	1.77	2625.1	103.1	1.63
2	15	4397.7	519.0	13.71	4408.7	358.8	1.75	4089.8	111.5	1.86
3	20	5595.6	441.5	14.14	5139.2	441.4	1.30	4335.6	381.4	2.13
4	25	8222.2	231.7	14.34	8187.2	227.8	1.47	5269.3	172.5	1.07
5	30	9053.3	255.8	18.32	9011.1	237.2	1.78	5704.5	207.7	1.81
Average		6088.4	405.2	14.39	5947.7	346.6	1.61	4404.8	195.2	1.70

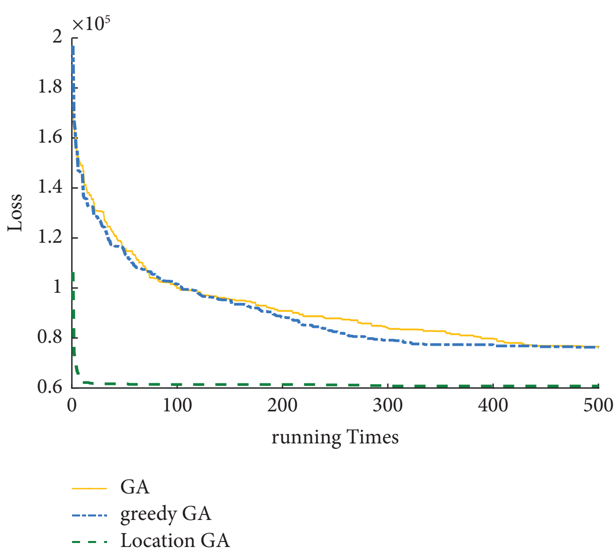

Figure 10: Comparison of the adaptation curves of the 3 algorithms.

traditional GA and GAA-GA algorithms converge from 200 generations, whereas the ALNS-GA algorithm converges much faster than the other two algorithms. Therefore, the ALNS-GA performs well in finding satisfactory solutions in small-scale cases.

5.4. Sensitivity Analysis

5.4.1. Drone Load Capacity Analysis. To test the effect of the drone load (*GD*) on the vehicle-drone joint distribution, *GD* is set to 20, 25, 30, 35, and 40, and the solution results are shown in Table 10.

From Figure 11, it can be seen that the change in drone load weight directly affects its flight cost and priority cost, which in turn affects the total cost of the entire process. As can be seen from Table 10, this process is based on meeting the range of the drone, and the original drone load capacity cannot meet the demand volume of all customer points or vehicle distribution; and with the increase in *GD*, the number of customer points that the drone can deliver increases. Thus, the drone flight cost also increases, and the speed of the drone is faster than the speed of the vehicle, which reduces the number of some customers who violate the soft time window limit, resulting in a priority cost reduction. Therefore, it is important to choose drones with a suitable load capacity; the price of the drone will not be too high at the same time, and the cost is reduced.

5.4.2. Drone Endurance Analysis. To test the impact of the drone range capacity (*LD*) on the vehicle-drone joint distribution, *LD* is set to 20, 25, 30, 35, and 40, and the solution results are shown in Table 11.

Table 10: Comparison of costs for different loads.

Load (*GD*)	20	25	30	35	40
Number of vehicles	7	6	5	5	4
Number of drones	4	4	5	5	4
Drone flight cost	310.9	316.7	321.4	339.7	377.0
Total cost of drone distribution	350.9	356.7	371.4	389.7	437.0
Vehicle driving cost	7051.7	6424.5	5539.9	5133.6	4968.1
Total costs of vehicle distribution	7751.7	7024.5	6039.9	5633.6	5368.1
Priority cost	3110.9	2476.7	1169.7	615.4	0
Total cost	11213.5	9587.9	7581.0	6638.7	5805.1

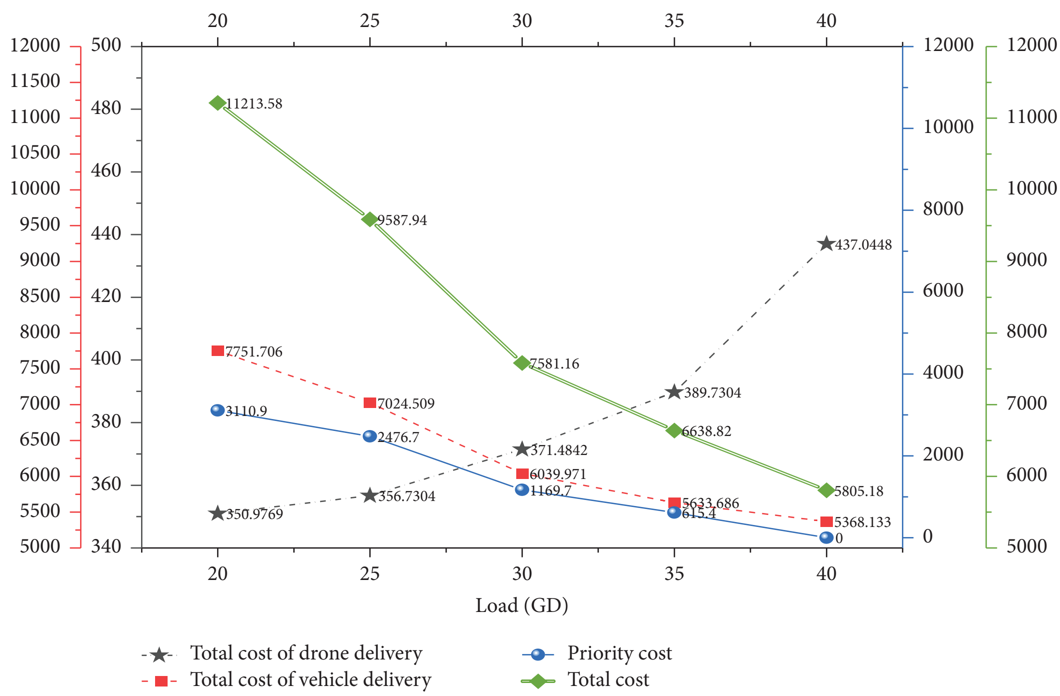

Figure 11: The change of each cost under different loadings.

Table 11: Comparison of costs for different endurance.

Endurance (*LD*)	20	25	30	35	40
Number of vehicles	6	5	5	5	4
Number of drones	3	4	5	5	4
Drone fixed cost	30	40	50	50	40
Drone flight cost	250.7	270.1	321.4	373.6	412.3
Total cost of drone delivery	280.7	310.1	371.4	423.6	452.3
Vehicle fixed cost	600	500	500	500	400
Vehicle driving cost	7433.9	6759.6	5539.9	5117.9	5045.4
Total cost of vehicle delivery	8033.9	7259.6	6039.9	5617.9	5445.4
Priority cost	2209.6	1676.7	1169.7	747.7	537.5
Total cost	10524.2	9246.4	7581.0	6789.2	6335.2

From Figure 12, it can be seen that the change in the range capacity of the drone directly affects the total cost of vehicle distribution, the cost of drone distribution, and the cost of priority, which in turn affects the total cost of the entire process. As shown in Table 11, in this process based on satisfying the range capacity, the drone cannot meet the demand quantity of all customer points at the beginning, and thus the number of drones used is small. In contrast, with the gradual increase in *LD*, the number of customer points that can be delivered increases, and the number of drones increases, which in turn increases the flight cost of drones and reduces the driving cost of vehicles, and the speed of drones is faster than that of vehicles. An increase in the number of drones used will reduce the number of customers who violate the soft time window limit, which leads to a reduction in priority cost. Therefore, as far as possible, to choose the appropriate endurance of the drone, the price of the drone will not be too high at the same time, and the cost will be reduced.

5.5. Whether to Consider Priority Comparison Analysis. A comparison between considering and not considering priority is shown in Figure 13. The solution results are shown in Table 12. When priority is not considered, the total cost of vehicle delivery is smaller than that when priority is considered, which proves that in order to meet the time window of customers with high priority as much as possible, the number of vehicles and drones will be increased, and the

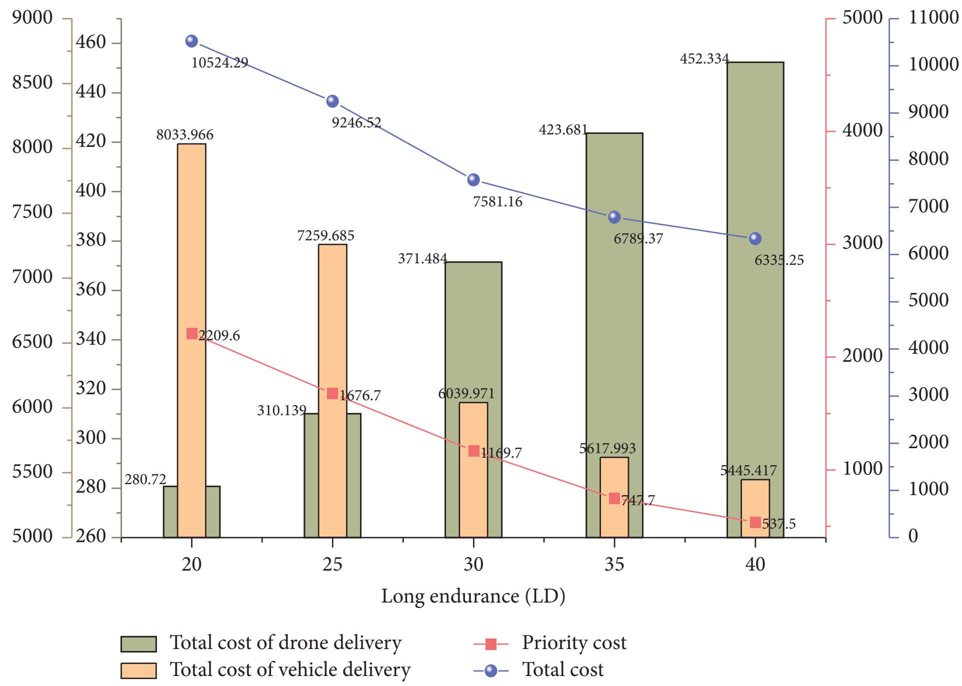

Figure 12: The change of each cost under different endurance.

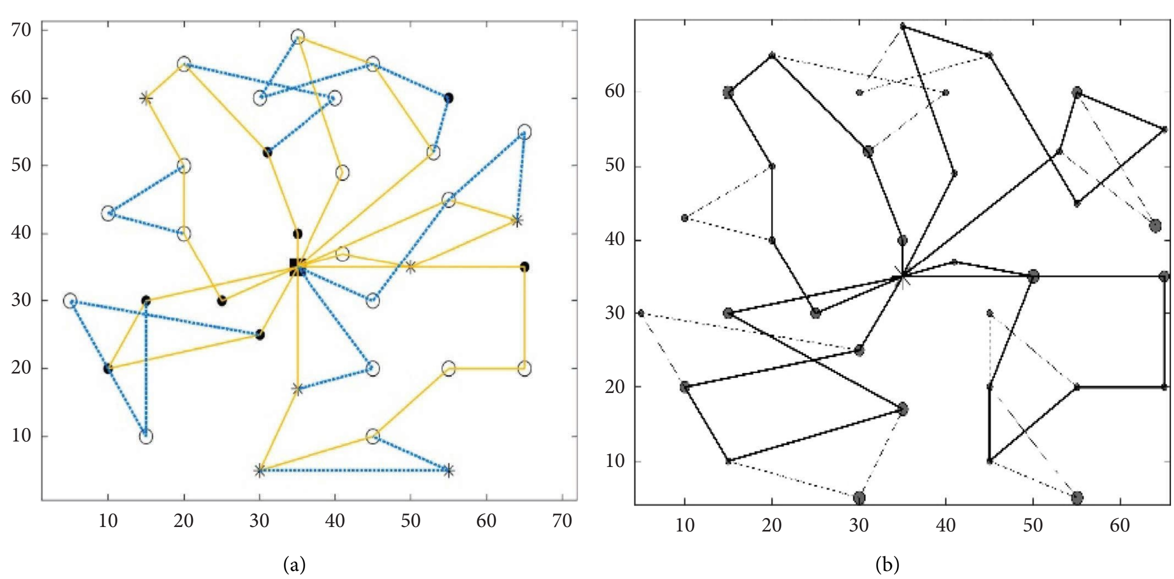

Figure 13: Comparison of routes (a) considering priority and (b) not considering priority.

Table 12: Comparison between considering priority and mot considering priority.

	No consideration of customer priorities	Consider the priority	Rate of change (%)
Number of vehicles	4	5	25.0
Number of drones	4	5	25.0
Vehicle travel distance	555.2	553.9	−0.2
Drone flight distance	285.2	321.4	12.7
Total cost of vehicle delivery	5952.3	6039.9	1.4
Total cost of drone delivery	325.2	371.4	14.2
Cost of lost satisfaction	1505.0	1169.7	−22.3
Total cost	7782.6	7581.0	−2.6

Table 13: Comparison of costs for different distribution scenarios.

Scenario	Total vehicle distribution cost	Total drone distribution cost	Number of distribution vehicles	Number of distribution drones	Number of unserved customers
1	7369.7	—	7	—	0
2	—	179.3	—	9	23
3	6039.9	371.4	5	5	0

vehicles and drones will travel a longer distance, which will lead to an increase in the total cost of vehicle delivery and drone delivery. If the priority is not considered, it leads to an increase in the cost of satisfaction loss. Finally, the total cost with the priority level considered is reduced by 2.6% compared to the total cost without the priority level. Therefore, customer priority can be considered in the distribution process, which increases the total distribution cost of vehicles and drones but reduces the satisfaction loss cost and the final total cost.

5.6. Different Distribution Scenarios Analysis. The vehicle-drone joint distribution (Scenario 3) is compared with the only vehicle distribution (Scenario 1) and the only drone distribution (Scenario 2). All three scenarios are analyzed under the premise of considering customer priority. A detailed comparison is shown in Table 13. In Scenario 1, one-to-one vehicle distribution to all customers creates long transport times and generates a higher total vehicle distribution cost. In Scenario 2, only drones are involved in distribution, which requires multiple drones to participate in distribution and cannot deliver customers beyond the longest flight distance due to the limitation of the flight distance and load capacity of drones. This results in many customers not being served, significantly reducing customer satisfaction, generating high-value loss, and being unrealistic. Scenario 3 involved the vehicle-drone joint distribution mode. The results show that vehicle-drone joint distribution can reduce the total cost and priority cost and verify that the vehicle-drone joint distribution considering customer priority can effectively reduce the distribution cost and deliver all customers.

6. Conclusion

This study investigates the path optimization problem of vehicle-drone joint distribution considering customer priorities and concludes the following:

(1) The DNN-GSM-SVM model was used to screen five main influencing features from 20 features, classify customer points into three priority classes, with a final MSE = 0.1421 variance loss indicator to prove the superiority of the classification model, and design the priority cost function that incorporates soft time windows for path optimization.

(2) By comparing the results of the traditional GA, GAA-GA, and ALNS-GA algorithms, the ALNS-GA optimizes the generation of satisfactory solutions and can obtain high-quality solutions in a shorter period, which proves the superiority of the algorithm. Through the sensitivity analysis of the drone load capacity and endurance, the drone with moderate load capacity and endurance is selected to reduce the cost, while the price of the drone will not be too high.

(3) By comparing the joint distribution with and without considering priority, it is found that customer priority should be considered. However, it increases the total delivery cost of vehicles and drones by a small amount, decreases the priority cost, and lowers the total cost.

(4) Finally, the different scenarios are compared, and it is found that only vehicle distribution generates a higher total cost. Only drone distribution cannot serve all customers, further validating the superiority of the vehicle-drone joint distribution.

The study will enrich the research on vehicle-drone joint distribution path optimization, provide a new theoretical basis and algorithm reference for how enterprises make decisions on customer priority, and provide a strong support and reference basis for vehicle-drone path planning aspects considering customer priority. In terms of actual complex road conditions, further studies on customer dynamic demands and drone charging cost can be considered in model construction in the future.

Data Availability

The path optimization data and priority data used to support the findings of this study are included within the supplementary information files.

Conflicts of Interest

The authors declare that they have no conflicts of interest.

Acknowledgments

This work was supported by the Liaoning Social Science Foundation under Grant L22ZD010.

Supplementary Materials

Two supplementary documents are data on path optimization and indicator data for evaluating priority. Among them, the data for path optimization were selected from the Solomon database, and 34 sets of data were selected for path research. The data for evaluating indicators are to first select 20 initial indicators, then conduct indicator screening, and finally classify customers based on the selected indicators. (*Supplementary Materials*)

References

[1] C. C. Murray and A. G. Chu, "The flying sidekick traveling salesman problem: optimization of drone-assisted parcel delivery," *Transportation Research Part C: Emerging Technologies*, vol. 54, pp. 86–109, 2015.

[2] Y. S. Chang and H. J. Lee, "Optimal delivery routing with wider drone-delivery areas along a shorter truck-route," *Expert Systems with Applications*, vol. 104, pp. 307–317, 2018.

[3] Q. M. Ha, Y. Deville, and Q. D. Pham, "On the min-cost traveling salesman problem with drone," *Transportation Research Part C*, vol. 86, pp. 597–621, 2018.

[4] N. Boysen, D. Briskorn, S. Fedtke, and S. Schwerdfeger, "Drone delivery from trucks: drone scheduling for given truck routes," *Networks*, vol. 72, no. 4, pp. 506–527, 2018.

[5] A. M. Ham, "Integrated scheduling of m-truck, m-drone, and m-depot constrained by time-window, drop pickup, and m-visit using constraint programming," *Transportation Research Part C: Emerging Technologies*, vol. 91, pp. 1–14, 2018.

[6] A. Karak and K. Abdelghany, "The hybrid vehicle drone routing problem for pick-up and delivery services," *Transportation Research Part C: Emerging Technologies*, vol. 102, pp. 427–449, 2019.

[7] C. Wang and H. J. Lan, "An expressway based on TSP model for vehicle delivery service coordinated with truck+UAV," in *Proceedings of the 2019 IEEE International Conference on Systems., Man and Cybernetics (SMC)*, pp. 307–311, IEEE, Bari, Italy, July, 2019.

[8] M. Moshref-Javadi, S. Lee, and M. Winkenbach, "Design and evaluation of a multi-trip delivery model with truck and drones," *Transportation Research Part E: Logistics and Transportation Review*, vol. 136, Article ID 101887, 2020.

[9] D. Schermer, M. Moeini, and O. Wendt, "The drone-assisted traveling salesman problem with robot stations," in *Proceedings of the 53rd Hawaii International Conference on System Sciences*, pp. 1308–1317, Hawaii, HI, USA, January, 2020.

[10] M. Salama and S. Srinivas, "Joint optimization of customer location clustering and drone-based routing for last-mile deliveries," *Transportation Research Part C: Emerging Technologies*, vol. 114, pp. 620–642, 2020.

[11] Y. Q. Han, J. Q. Li, Z. M. Liu, C. Liu, and J. Tian, "Metaheuristic algorithm for solving the multi-objective vehicle routing problem with time window and drones," *International Journal of Advanced Robotic Systems*, vol. 17, no. 2, Article ID 172988142092003, 2020.

[12] Y. Peng and Y. J. Lai, "Collaborative truck-drone distribution path optimization considering the impact of epidemic," *Chinese Journal of Highways*, vol. 33, no. 11, pp. 73–82, 2020.

[13] I. Dayarian, M. Savelsbergh, and J. P. Clarke, "Same-day delivery with drone resupply," *Transportation Science*, vol. 54, no. 1, pp. 229–249, 2020.

[14] W. Liu, L. Wang, and Q. Zhou, "Optimization model and algorithm for"UAV-vehicle"distribution path," *Transportation Systems Engineering and Information*, vol. 21, no. 6, pp. 176–186, 2021.

[15] R. Yan, L. S. Chen, and X. N. Zhu, "Research on truck-mounted UAV vehicle path problem considering regional restrictions," *China Management Science*, vol. 30, no. 5, pp. 144–155, 2022.

[16] S. Yang, X. Guo, and J. Gao, "Research on contactless"truck+drone"co-delivery," *Industrial Engineering & Management*, vol. 27, no. 1, pp. 184–194, 2022.

[17] J. Zhang and Y. F. Li, "The site-path problem of fresh food distribution in the epidemic environment," *China Management Science*, pp. 1–12, 2023.

[18] T. S. M. Windras, S. Ruhul, and E. Daryl, "Solving electric vehicle–drone routing problem using memetic algorithm," *Swarm and Evolutionary Computation*, vol. 79, 2023.

[19] X. Wang, S. Poikonen, and B. Golden, "The vehicle routing problem with drones: several worst-case results," *Optimization Letters*, vol. 11, no. 4, pp. 679–697, 2017.

[20] S. Poikonen, X. Wang, and B. Golden, "The vehicle routing problem with drones: extended models and connections," *Networks*, vol. 70, no. 1, pp. 34–43, 2017.

[21] D. Schermer, M. Moeini, and O. Wendt, "A hybrid VNS/Tabu search algorithm for solving the vehicle routing problem with drones and en route operations," *Computers and Operations Research*, vol. 109, pp. 134–158, 2019.

[22] D. Popovic, M. Kovac, and N. Bjelic, "A miqp model for solving the vehicle routing problem with drones," in *Proceedings of the 4th Logistics International Conference*, pp. 53–62, Rome, Italy, May, 2019.

[23] D. Sacramento, D. Pisinger, and S. Ropke, "An adaptive large neighborhood search metaheuristic for the vehicle routing problem with drones," *Transportation Research Part C: Emerging Technologies*, vol. 102, pp. 289–315, 2019.

[24] R. J. Kuo, S. H. Lu, P. Y. Lai, and S. T. W. Mara, "Vehicle routing problem with drones considering time windows," *Expert Systems with Applications*, vol. 191, Article ID 116264, 2022.

[25] C. C. Murray and R. Raj, "The multiple flying sidekicks traveling salesman problem: parcel delivery with multiple drones," *Transportation Research Part C: Emerging Technologies*, vol. 110, pp. 368–398, 2020.

[26] T. Zhu, S. D. Boyles, and A. Unnikrishnan, "Electric vehicle traveling salesman problem with drone with partial recharge policy," pp. 1–34, 2022, https://arxiv.org/abs/2205.13735.

[27] N. A. Kyriakakis, T. Stamadianos, M. Marinaki, and Y. Marinakis, "The electric vehicle routing problem with drones: an energy minimization approach for aerial deliveries," *Cleaner Logistics and Supply Chain*, vol. 4, Article ID 100041, 2022.

[28] S. T. Windras Mara, A. P. Rifai, and B. M. Sopha, "An adaptive large neighborhood search heuristic for the flying sidekick traveling salesman problem with multiple drops," *Expert Systems with Applications*, vol. 205, Article ID 117647, 2022.

[29] R. M. De Souza, R. Morabito, F. Y. Chiyoshi, and A. P. Iannoni, "Incorporating priorities for waiting customers in the hypercube queuing model with application to an emergency medical service system in Brazil," *European Journal of Operational Research*, vol. 242, no. 1, pp. 274–285, 2015.

[30] J. S. H. Lee, D. McCole, and D. Holecek, "Exploring winery visitors in the emerging wine regions of the north Central United States," *Sustainability*, vol. 12, no. 4, p. 1642, 2020.

[31] J. B. Schreiber, "Issues and recommendations for exploratory factor analysis and principal component analysis," *Research in Social and Administrative Pharmacy*, vol. 17, no. 5, pp. 1004–1011, 2021.

[32] F. Wang, Y. Lu, J. Li, and J. Ni, "Evaluating environmentally sustainable development based on the PSR framework and variable weigh analytic hierarchy process," *International Journal of Environmental Research and Public Health*, vol. 18, no. 6, p. 2836, 2021.

[33] N. Shrestha, "Factor analysis as a tool for survey analysis," *American Journal of Applied Mathematics and Statistics*, vol. 9, no. 1, pp. 4–11, 2021.